

Radiative Decays of the $\Upsilon(1S)$ to a Pair of Charged Hadrons*

S. B. Athar,¹ P. Avery,¹ L. Brevva-Newell,¹ R. Patel,¹ V. Potlia,¹ H. Stoeck,¹ J. Yelton,¹
P. Rubin,² C. Cawfield,³ B. I. Eisenstein,³ G. D. Gollin,³ I. Karliner,³ D. Kim,³ N. Lowrey,³
P. Naik,³ C. Sedlack,³ M. Selen,³ E. J. White,³ J. Williams,³ J. Wiss,³ K. W. Edwards,⁴
D. Besson,⁵ T. K. Pedlar,⁶ D. Cronin-Hennessy,⁷ K. Y. Gao,⁷ D. T. Gong,⁷ J. Hietala,⁷
Y. Kubota,⁷ T. Klein,⁷ B. W. Lang,⁷ S. Z. Li,⁷ R. Poling,⁷ A. W. Scott,⁷ A. Smith,⁷
S. Dobbs,⁸ Z. Metreveli,⁸ K. K. Seth,⁸ A. Tomaradze,⁸ P. Zweber,⁸ J. Ernst,⁹ K. Arms,¹⁰
H. Severini,¹¹ D. M. Asner,¹² S. A. Dytman,¹² W. Love,¹² S. Mehrabyan,¹² J. A. Mueller,¹²
V. Savinov,¹² Z. Li,¹³ A. Lopez,¹³ H. Mendez,¹³ J. Ramirez,¹³ G. S. Huang,¹⁴
D. H. Miller,¹⁴ V. Pavlunin,¹⁴ B. Sanghi,¹⁴ I. P. J. Shipsey,¹⁴ G. S. Adams,¹⁵ M. Cravey,¹⁵
J. P. Cummings,¹⁵ I. Danko,¹⁵ J. Napolitano,¹⁵ Q. He,¹⁶ H. Muramatsu,¹⁶ C. S. Park,¹⁶
E. H. Thorndike,¹⁶ T. E. Coan,¹⁷ Y. S. Gao,¹⁷ F. Liu,¹⁷ R. Stroynowski,¹⁷ M. Artuso,¹⁸
C. Boulahouache,¹⁸ S. Blusk,¹⁸ J. Butt,¹⁸ O. Dorjkhaidav,¹⁸ J. Li,¹⁸ N. Menea,¹⁸
R. Mountain,¹⁸ R. Nandakumar,¹⁸ K. Randrianarivony,¹⁸ R. Redjimi,¹⁸ R. Sia,¹⁸
T. Skwarnicki,¹⁸ S. Stone,¹⁸ J. C. Wang,¹⁸ K. Zhang,¹⁸ S. E. Csorna,¹⁹ G. Bonvicini,²⁰
D. Cinabro,²⁰ M. Dubrovin,²⁰ A. Bornheim,²¹ S. P. Pappas,²¹ A. J. Weinstein,²¹
R. A. Briere,²² G. P. Chen,²² J. Chen,²² T. Ferguson,²² G. Tatishvili,²² H. Vogel,²²
M. E. Watkins,²² J. L. Rosner,²³ N. E. Adam,²⁴ J. P. Alexander,²⁴ K. Berkelman,²⁴
D. G. Cassel,²⁴ V. Crede,²⁴ J. E. Duboscq,²⁴ K. M. Ecklund,²⁴ R. Ehrlich,²⁴ L. Fields,²⁴
R. S. Galik,²⁴ L. Gibbons,²⁴ B. Gittelman,²⁴ R. Gray,²⁴ S. W. Gray,²⁴ D. L. Hartill,²⁴
B. K. Heltsley,²⁴ D. Hertz,²⁴ C. D. Jones,²⁴ J. Kandaswamy,²⁴ D. L. Kreinick,²⁴
V. E. Kuznetsov,²⁴ H. Mahlke-Krüger,²⁴ T. O. Meyer,²⁴ P. U. E. Onyisi,²⁴
J. R. Patterson,²⁴ D. Peterson,²⁴ E. A. Phillips,²⁴ J. Pivarski,²⁴ D. Riley,²⁴ A. Ryd,²⁴
A. J. Sadoff,²⁴ H. Schwarthoff,²⁴ X. Shi,²⁴ M. R. Shepherd,²⁴ S. Stroiney,²⁴
W. M. Sun,²⁴ D. Urner,²⁴ T. Wilksen,²⁴ K. M. Weaver,²⁴ and M. Weinberger²⁴

(CLEO Collaboration)

¹*University of Florida, Gainesville, Florida 32611*

²*George Mason University, Fairfax, Virginia 22030*

³*University of Illinois, Urbana-Champaign, Illinois 61801*

⁴*Carleton University, Ottawa, Ontario, Canada K1S 5B6
and the Institute of Particle Physics, Canada*

⁵*University of Kansas, Lawrence, Kansas 66045*

⁶*Luther College, Decorah, Iowa 52101*

⁷*University of Minnesota, Minneapolis, Minnesota 55455*

⁸*Northwestern University, Evanston, Illinois 60208*

⁹*State University of New York at Albany, Albany, New York 12222*

¹⁰*Ohio State University, Columbus, Ohio 43210*

¹¹*University of Oklahoma, Norman, Oklahoma 73019*

¹²*University of Pittsburgh, Pittsburgh, Pennsylvania 15260*

¹³*University of Puerto Rico, Mayaguez, Puerto Rico 00681*

¹⁴*Purdue University, West Lafayette, Indiana 47907*

¹⁵*Rensselaer Polytechnic Institute, Troy, New York 12180*

¹⁶*University of Rochester, Rochester, New York 14627*

¹⁷*Southern Methodist University, Dallas, Texas 75275*

¹⁸*Syracuse University, Syracuse, New York 13244*

¹⁹*Vanderbilt University, Nashville, Tennessee 37235*

²⁰*Wayne State University, Detroit, Michigan 48202*

²¹*California Institute of Technology, Pasadena, California 91125*

²²*Carnegie Mellon University, Pittsburgh, Pennsylvania 15213*

²³*Enrico Fermi Institute, University of Chicago, Chicago, Illinois 60637*

²⁴*Cornell University, Ithaca, New York 14853*

(Dated: June 19, 2005)

Abstract

Using data obtained with the CLEO III detector, running at the Cornell Electron Storage Ring (CESR), we report on a new study of exclusive radiative $\Upsilon(1S)$ decays into the final states $\gamma\pi^+\pi^-$, γK^+K^- , and $\gamma p\bar{p}$. We present branching ratio measurements for the decay modes $\Upsilon(1S) \rightarrow \gamma f_2(1270)$, $\Upsilon(1S) \rightarrow \gamma f_2'(1525)$, and $\Upsilon(1S) \rightarrow \gamma K^+K^-$; helicity production ratios for $f_2(1270)$ and $f_2'(1525)$; upper limits for the decay $\Upsilon(1S) \rightarrow \gamma f_J(2200)$, with $f_J(2220) \rightarrow \pi^+\pi^-$, K^+K^- , $p\bar{p}$; and an upper limit for the decay $\Upsilon(1S) \rightarrow \gamma X(1860)$, with $X(1860) \rightarrow \gamma p\bar{p}$.

*Submitted to the XXII International Symposium on Lepton and Photon Interactions at High Energies, June 30-July 5, 2005, Uppsala, Sweden

I. INTRODUCTION

Radiative decays of heavy-quarkonia, where a photon replaces one of the three gluons from the strong decay of, for example, the J/ψ or $\Upsilon(1S)$, are useful in studying color-singlet two-gluon systems. The two gluons can, among other things, hadronize into a meson¹, or directly form a glueball². Further information on radiative decays of heavy-quarkonia can be found in [39].

Light meson production in J/ψ two-body radiative decays has been experimentally well established at the 10^{-3} level, based largely on evidence provided by radiative decays to a pair of hadrons³. Helicity production ratio measurements have been made for the tensor mesons $f_2(1270)$ [41–44] and $f_2'(1525)$ [45, 46] in J/ψ two-body radiative decays and agree with theoretical predictions [47, 48]. In 1996, the BES collaboration claimed to observe the $f_J(2220)$ in J/ψ two-body radiative decays, and measured product branching fractions, $\mathcal{B}(J/\psi \rightarrow \gamma f_J(2220)) \times \mathcal{B}(f_J(2220) \rightarrow h^+ h^-)$ (we use the convention $h = \pi, K, p$), of the order of 10^{-5} [49]. Much excitement was generated at the time because it is possible to interpret the $f_J(2220)$ as a glueball. A candidate similar to $f_J(2220)$ was reported in 1986 by the Mark III collaboration in the $K\bar{K}$ mode [50], but was not confirmed by the DM2 collaboration [51]. Recently, BES has claimed to observe the signal candidate $X(1860)$ via $J/\psi \rightarrow \gamma X(1860) \rightarrow p\bar{p}$ [52], a result that is currently being interpreted [53–59].

The experimental observation of radiative $\Upsilon(1S)$ decays is challenging because their rate is suppressed by a factor of the order of,

$$\left(\frac{q_b}{q_c}\right)^2 \left(\frac{m_c}{m_b}\right)^2 \approx 0.025,$$

with respect to the rate of J/ψ radiative decays. This factor arises because the quark-photon coupling is proportional to the electric charge, and the quark propagator is roughly proportional to $1/m$ for low momentum quarks. Taking into account the total widths [40] of J/ψ and $\Upsilon(1S)$, the branching fraction of a particular $\Upsilon(1S)$ radiative decay mode is expected to be suppressed by a factor of roughly 0.04. In 1999 CLEO II made the first observation of a radiative $\Upsilon(1S)$ decay to a pair of hadrons [60], which was consistent with $\Upsilon(1S) \rightarrow \gamma f_2(1270)$, where $f_2(1270) \rightarrow \pi\pi$. Comparing the measured branching fraction to the $J/\psi \rightarrow \gamma f_2(1270)$ branching fraction, a suppression factor of 0.06 ± 0.03 was obtained. Recent theoretical works [2, 3], predict a suppression factor between 0.06 – 0.18 for this mode, and favor the production of $f_2(1270)$ in a helicity 0 state. After the BES result for

¹ Several authors have studied meson production in $\Upsilon(1S)$ radiative decays, giving predictions for branching and helicity production ratios. The heavy-quarkonia system is usually described by non-relativistic QCD [1], while the gluonic hadronization has been treated using soft collinear effective theory [2], gluon distribution amplitudes [3], and perturbative QCD [4, 5].

² Glueballs are a natural consequence of QCD, and predictions of their properties have been made using different approaches, such as, potential models [6–8], lattice QCD calculations [9–12], bag models [13–16], flux-tube models [17], the QCD sum rule [18], the Bethe-Salpeter (B-S) equation [19, 20], QCD factorization formalism models [21, 22], weakly-bound-state models [23], and a three-dimensional relativistic equation [24]. However, despite intense experimental searches [25–30], there is no conclusive experimental evidence of their observation, although there are strong indications that glueballs contribute to the rich light scalar spectrum [31–38].

³ We refer to the Particle Data Group [40] for a summary of J/ψ radiative decays.

the $f_J(2220)$ in radiative J/ψ decays, a corresponding search was performed by CLEO II in the radiative $\Upsilon(1S)$ system [61] and limits were put on some of the glueball candidate's product branching ratios.

In this paper, we use a new CLEO III $\Upsilon(1S)$ data sample, which has fifteen times higher statistics and better particle identification than the CLEO II data sample, to probe the color-singlet two-gluon spectrum by measuring the system's invariant mass using its decays to $\pi^+\pi^-$, K^+K^- , and $p\bar{p}$. Further details of this analysis can be found elsewhere [62].

II. CLEO III DETECTOR, DATA, AND MONTE CARLO SIMULATED SAMPLE

The CLEO III detector is a versatile multi-purpose particle detector described more fully in [63]. It is centered on the interaction region of CESR. From the e^+e^- interaction region radially outward it consists of a silicon strip vertex detector and a wire drift chamber used to measure the position, momenta, and ionization energy losses (dE/dx) of charged tracks based on their fitted path in a 1.5 T solenoidal magnetic field and the amount of charge deposited on the drift chamber wires. The silicon vertex detector and drift chamber tracking system achieves a charged particle momentum resolution of 0.35%(1%) at 1 GeV/c(5 GeV/c) and a dE/dx resolution of 6%. Beyond the drift chamber is a Ring Imaging Cherenkov Detector, RICH, which covers 80% of the solid angle and is used to further identify charged particles by giving for each mass hypothesis the likelihood of a fit to the Cherenkov radiation pattern. After the RICH is a Crystal Calorimeter (CC) that covers 93% of the solid angle. The CC has a resolution of 2.2%(1.5%) for 1 GeV(5 GeV) photons. After the CC is a superconducting solenoid coil that provides the magnetic field, followed by iron flux return plates with wire chambers interspersed in three layers at 3, 5, and 7 hadronic interaction lengths to provide muon identification.

The data sample has an integrated luminosity of 1.13 fb^{-1} taken at the $\Upsilon(1S)$ energy, $\sqrt{s} = 9.46 \text{ GeV}$, which correspond to 21.2 ± 0.2 million $\Upsilon(1S)$ decays [64] and 3.49 fb^{-1} taken at the $\Upsilon(4S)$ energy, $\sqrt{s} = 10.56 \text{ GeV}$, used to model the underlying continuum present in the $\Upsilon(1S)$ data sample. The continuum background modeling is important because continuum background processes such as $e^+e^- \rightarrow \gamma\rho$ with $\rho \rightarrow \pi^+\pi^-$, $e^+e^- \rightarrow \gamma\phi$ with $\phi \rightarrow K^+K^-$, and direct $e^+e^- \rightarrow \gamma h^+h^-$, have the same topology as the signal events we are investigating.

Efficiencies are evaluated using a Monte Carlo simulation of the process [65] and a GEANT-based [66] detector response. Monte Carlo samples of $e^+e^- \rightarrow \gamma X$ with $X \rightarrow h^+h^-$ are generated [67] at both the $\Upsilon(1S)$ and $\Upsilon(4S)$ energies with uniform angular distributions and flat h^+h^- invariant mass distributions from threshold to $3.5 \text{ GeV}/c^2$.

III. EVENT SELECTION

Events which satisfy the CLEO III trigger [68] are required to meet the following analysis requirements: (a) There are exactly two charged tracks consistent with coming from the beamspot, with dE/dx information, and with good quality track fits. (b) There is exactly one CC shower that is unmatched to any track and whose energy, E_γ , is greater than 4 GeV.

Each event is also required to be consistent with having the 4-momentum of the initial e^+e^- system by demanding that the chi-squared from a kinematic fit to the following constraint,

$$\vec{p}_{h^+h^-} + (2E_{beam} - E_{h^+h^-})\hat{p}_\gamma = \vec{p}_{CM}, \quad (1)$$

be less than 100, where \vec{p}_{h+h^-} is the di-hadron momentum, E_{h+h^-} is the di-hadron energy, E_{beam} is the beam energy, \hat{p}_γ is the photon's direction, and \vec{p}_{CM} is the momentum of the e^+e^- system (which has a magnitude of a few MeV/c because of the small but finite crossing angle of the e^+ and e^- beams). Equation 1 is a 3-constraint subset of the 4-momentum constraint and has the convenient property of avoiding the use of the measured photon's energy, which has an asymmetric measurement error. We improve the measurement of the di-hadron 4-momenta (the di-hadron invariant mass resolution becomes 3.2, 2.6, and 2.0 MeV/c² for the pion, kaon, and proton modes, respectively) by using the constraint in equation 1, and then demand that:

$$0.950 < (E_{h+h^-} + E_\gamma)/2E_{beam} < 1.025.$$

Strong electron and muon vetoes are imposed to suppress the abundant QED processes $e^+e^- \rightarrow \gamma e^+e^-$ and $e^+e^- \rightarrow \gamma\mu^+\mu^-$. To reject $e^+e^- \rightarrow \gamma e^+e^-$, we require each track to have a matched CC shower with an energy E , together with a measured momentum p , such that $|E/p - 0.95| > 0.1$, and that the combined RICH and dE/dx likelihood for h be higher than the combined likelihood for e . To reject $e^+e^- \rightarrow \gamma\mu^+\mu^-$, we require that neither track produce a signal in the five hadronic interaction lengths of the muon system. For the $\pi^+\pi^-$ mode, where muon background is a particular problem because of the similar pion and muon masses, we further require that both tracks must be within the barrel part of the muon chambers ($|\cos\theta| < 0.7$), and both have $p > 1$ GeV/c. To increase the solid-angle acceptance of the detector and improve the overall muon suppression efficiency with virtually no increase in muon fakes, we flag an event as “not muonic” and remove the muon suppression requirements if either track deposits more than 600 MeV in the CC.

Events that satisfy all the above requirements are then identified as either $\pi^+\pi^-$, K^+K^- , or $p\bar{p}$ using the RICH and dE/dx information. Since the ratios $\pi^+\pi^-/K^+K^-$ and $K^+K^-/p\bar{p}$ are much larger than 1 for these types of events, in the 3 cases where we try to reduce the background from a lower-mass hadron (e.g. π faking K), we also use the chi-squared value from the kinematic constraint in Equation 1 to identify the event type. Since the constraint involves the di-hadron energy, the chi-squared value is sensitive to the hadronic masses. After these procedures, the particle identification and fake rates are 90% (0.31%), 99% (0.03%), 98% (0.10%) for kaons (pions), protons (pions), and protons (kaons), respectively.

IV. DETERMINATION OF SIGNALS AND THEIR SPIN ASSIGNMENTS

The overall reconstruction efficiencies as determined by Monte Carlo simulations, including both event selection and analysis cuts, are 43%, 48%, and 56% for the $\Upsilon(1S)$ radiative decays to $\pi^+\pi^-$, K^+K^- , and $p\bar{p}$, respectively. These efficiencies are only mildly dependent on the di-hadron invariant mass and are very similar for the continuum background events. The continuum subtracted di-hadron invariant mass plots are obtained by efficiency correcting each bin of the di-hadron invariant mass plots for the $\Upsilon(1S)$ and $\sqrt{s} = 10.56$ GeV datasets, scaling the latter plot by a factor of 0.404 ± 0.002^4 , and subtracting it from the $\Upsilon(1S)$ dataset invariant mass plot. Possible signals are determined by fitting each spectrum to spin-dependent relativistic Breit-Wigner functions⁵. The spin value for each Breit-Wigner

⁴ We obtain this factor, f , from the integrated luminosities of the the $\Upsilon(1S)$ and $\sqrt{s} = 10.56$ GeV datasets, and the assumption that, to first order, the cross sections of the continuum processes in each run are proportional to $1/s$. This factor is roughly equal to E_γ the factor obtained by using the average energy of

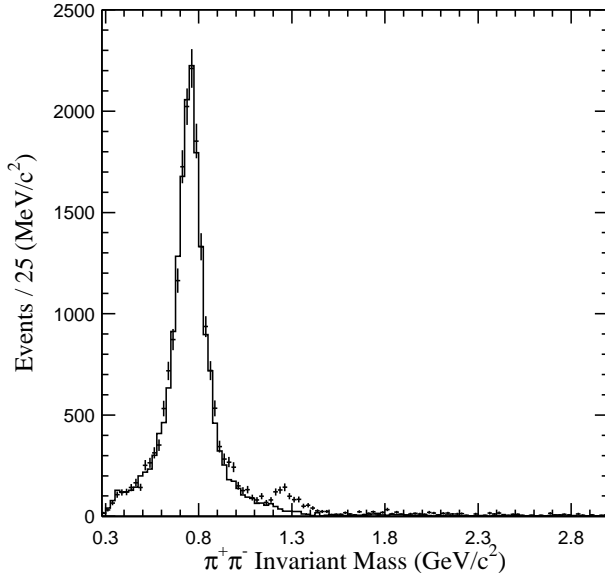


FIG. 1: Invariant mass of $\pi^+\pi^-$ from $e^+e^- \rightarrow \gamma\pi^+\pi^-$ for the scaled $\sqrt{s} = 10.56$ GeV dataset (solid line), and the $\Upsilon(1S)$ dataset (crosses). The large number of events near 770 MeV/ c^2 is due to the abundant process $e^+e^- \rightarrow \gamma\rho$.

is surmised by identifying each possible resonance in the invariant mass plot based on its approximate mass and width. Later, we confirm these spin assignments for the significant resonances by inspecting the angular distributions of the $\Upsilon(1S)$ decay products.

The $\pi^+\pi^-$ invariant mass plots for the $\Upsilon(1S)$ and the scaled $\sqrt{s} = 10.56$ GeV datasets are shown in Figure 1. The fit to the continuum subtracted $\pi^+\pi^-$ spectrum, shown in Figure 2, has a significant $f_2(1270)$ signal of 944 ± 74 events. It also has two less significant signal candidates; 340^{+140}_{-130} events in the $f_0(980)$ region, and 80 ± 30 events in the $f_4(2050)$ region (see Figure 3) whose significances are 4.3σ and 2.6σ , respectively. Each significance

each dataset,

$$f = 0.404 \approx \frac{1.13 \text{ fb}^{-1}}{3.49 \text{ fb}^{-1}} \left(\frac{10.56 \text{ GeV}}{9.46 \text{ GeV}} \right)^2.$$

⁵ The spin-dependent relativistic Breit-Wigner parameterization used has the following probability distribution for a particular h^+h^- invariant mass $x > x_0$,

$$dP(x) \propto \frac{xx_m\Gamma(x)}{(x^2 - x_m^2)^2 + (x_m\Gamma(x))^2} dx,$$

where:

$$\Gamma(x) = \Gamma_0 \left(\frac{x - x_0}{x_m - x_0} \right)^{2S+1} \frac{2(x_m - x_0)^2}{(x - x_0)^2 + (x_m - x_0)^2}.$$

In the above expression, x_m and Γ_0 represent respectively the most likely mass and the width and are allowed to float during the fit. The values of x_0 and S are fixed during the fit to the invariant mass threshold for the particular mode and the spin of the resonance, respectively. The number of events for each fitted signal candidate is obtained by integrating this Breit-Wigner parameterization between threshold and 3 GeV/ c^2 .

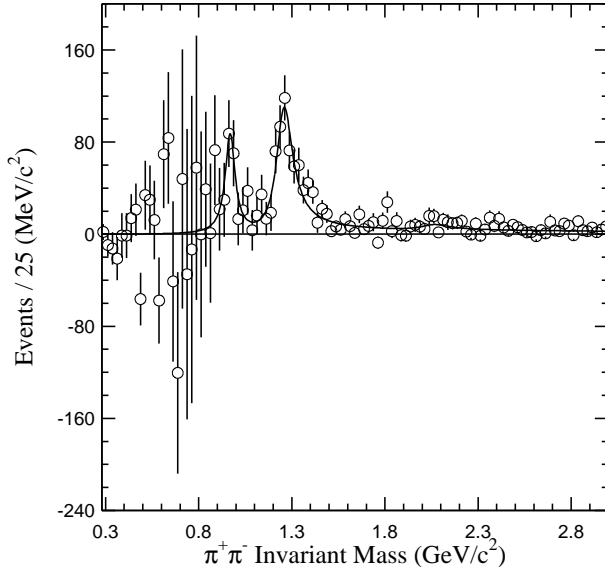


FIG. 2: Invariant mass of $\pi^+\pi^-$ from $\Upsilon(1S) \rightarrow \gamma\pi^+\pi^-$ and the fit to the three spin-dependent relativistic Breit-Wigner functions described in the text.

is obtained by doing multiple chi-squared fits to the invariant mass plot fixing the signal area to different values, assigning each of these multiple fits a probability proportional to $e^{-\chi^2/2}$, normalizing the resulting probability distribution, and calculating the probability for negative or 0 signal. The K^+K^- invariant mass plots for the $\Upsilon(1S)$ and the scaled $\sqrt{s} = 10.56$ GeV datasets are shown in Figure 4. The fit to the continuum subtracted K^+K^- spectrum, shown in Figure 5, has a significant signal of 312^{+69}_{-61} events identified as the $f'_2(1525)$, and two non-significant signal candidates indicating possible $f_2(1270)$ and $f_0(1710)$ production with 109 ± 36 and 73 ± 29 events whose significances are 3.2σ and 3.3σ , respectively. The excess in the $f_2(1270)$ region is consistent with that expected using the $\gamma\pi^+\pi^-$ data and the known branching ratios for the $f_2(1270)$. We also note that there is a significant excess of 220 ± 20 events above 1.9 GeV in the K^+K^- invariant mass distribution which is not associated with any resonant structure. The $p\bar{p}$ invariant mass plots for the $\Upsilon(1S)$ and the scaled $\sqrt{s} = 10.56$ GeV datasets are shown in Figure 6. No recognizable structure is seen in the continuum subtracted $p\bar{p}$ spectrum, which is shown in Figure 7, and has an excess of 85 ± 18 events in the $2 - 3$ GeV/ c^2 invariant mass region. In particular, we do not note a significant enhancement near threshold.

To confirm the spins of our $f_2(1270) \rightarrow \pi^+\pi^-$ and $f'_2(1525) \rightarrow K^+K^-$ signals, we examine the absolute value of the cosine of the polar angle of the photon with respect to the beam axis, $|\cos\theta_\gamma|$, and the absolute value of the cosine of the angle formed by the 3-momentum vector of one of the hadrons measured in the di-hadron rest frame with the photon's direction, $|\cos\theta_h|$. The event selection efficiency is slightly dependent on both angles, so to minimize systematic effects, the $|\cos\theta_\gamma|$ and $|\cos\theta_h|$ efficiency-corrected distributions are obtained by projecting the 2-dimensional bin-by-bin efficiency-corrected $|\cos\theta_\gamma|$ - $|\cos\theta_h|$ distribution. We also subtract the background contributions from the tails of nearby resonances. The resulting angular distributions (shown in Figures 8 and 9) are simultaneously fit to the helicity formalism prediction [48, 62, 69] for different resonance spin hypotheses up to $J = 4$. For the $f_2(1270)$ the different fit confidence levels are 8×10^{-19} , 2×10^{-19} , 0.05 , 8×10^{-12} ,

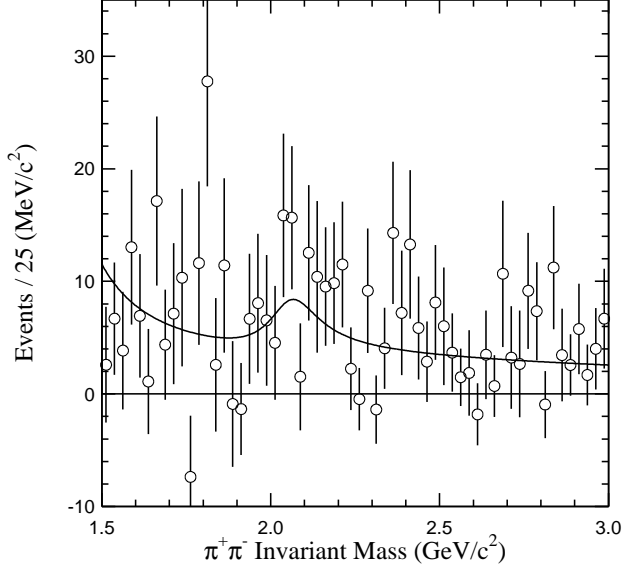


FIG. 3: Invariant mass of $\pi^+\pi^-$ from $\Upsilon(1S) \rightarrow \gamma\pi^+\pi^-$ and the fit to the $f_4(2050)$ candidate in the region $1.5\text{-}3.0\text{ GeV}/c^2$.

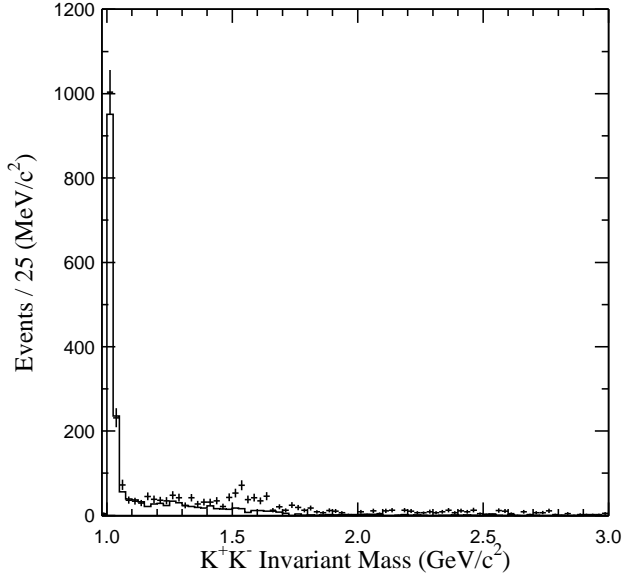


FIG. 4: Invariant mass of K^+K^- from $e^+e^- \rightarrow \gamma K^+K^-$ for the scaled $\sqrt{s} = 10.56\text{ GeV}$ dataset (solid line), and the $\Upsilon(1S)$ dataset (crosses). The large number of events near $1.050\text{ GeV}/c^2$ is due to the abundant process $e^+e^- \rightarrow \gamma\phi$.

and 1×10^{-12} for the hypotheses $J = 0, 1, 2, 3, 4$, respectively. For the $f_2'(1525)$ the different fit confidence levels are 2×10^{-4} , 2×10^{-4} , 0.23 , 8×10^{-3} , and 2×10^{-3} for the hypotheses $J = 0, 1, 2, 3, 4$, respectively. These results confirm our identification of the resonances, as

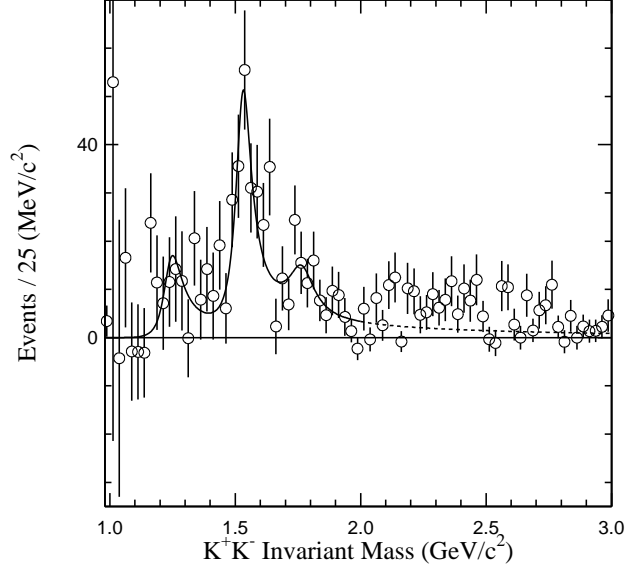


FIG. 5: Invariant mass of K^+K^- from $\Upsilon(1S) \rightarrow \gamma K^+K^-$ and the fit to the three spin-dependent relativistic Breit-Wigner functions described in the text.

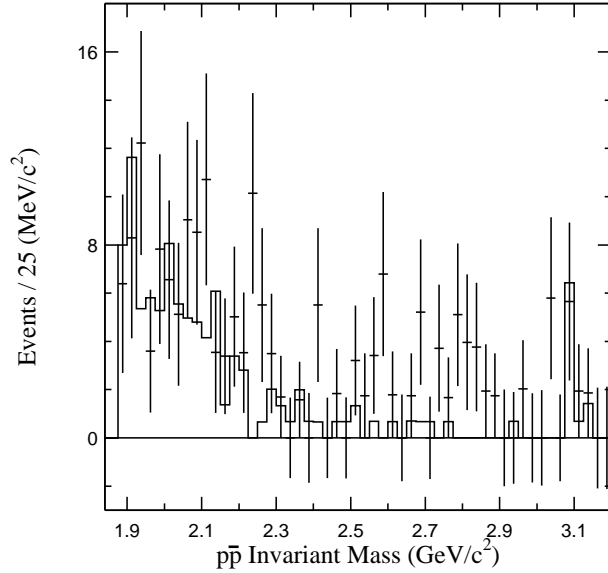


FIG. 6: Invariant mass of $p\bar{p}$ from $e^+e^- \rightarrow \gamma p\bar{p}$ for the scaled $\sqrt{s} = 10.56$ GeV dataset (solid line), and the $\Upsilon(1S)$ dataset (crosses). The events near 3.1 GeV/c² are due to the process $e^+e^- \rightarrow \gamma J/\psi$.

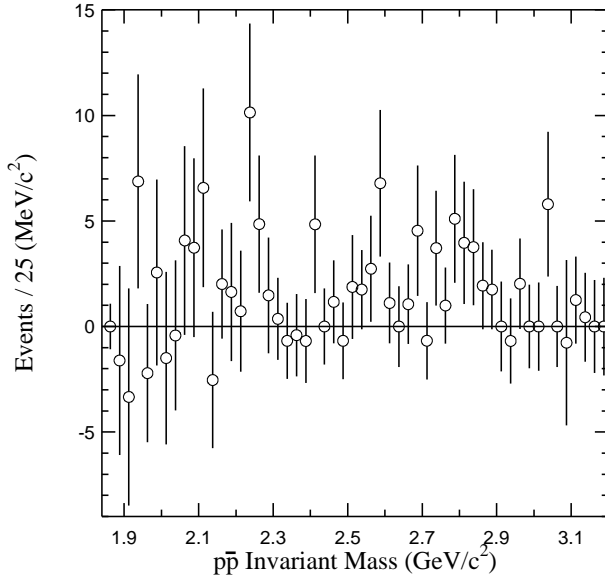


FIG. 7: Invariant mass of $p\bar{p}$ from $\Upsilon(1S) \rightarrow \gamma p\bar{p}$.

in both cases the angular distributions of the data strongly favor the $J = 2$ hypothesis⁶,

$$\begin{aligned} \frac{dP_{\theta_h, \theta_\gamma}}{d \cos \theta_h d \cos \theta_\gamma} &= |a_0|^2 \times \frac{5}{8} (3 \cos^2 \theta_h - 1)^2 \times \frac{3}{8} (1 + \cos^2 \theta_\gamma) + \\ &|a_1|^2 \times \frac{15}{16} \sin^2 2\theta_h \times \frac{3}{4} \sin^2 \theta_\gamma + \\ &|a_2|^2 \times \frac{15}{16} \sin^4 \theta_h \times \frac{3}{8} (1 + \cos^2 \theta_\gamma), \end{aligned} \quad (2)$$

where a_λ , $\lambda = 0, 1, 2$, are the normalized helicity amplitudes, $\int dP_{\theta_h, \theta_\gamma} = |a_0|^2 + |a_1|^2 + |a_2|^2 = 1$. In other words, $|a_\lambda|^2$ is the probability of X in $\Upsilon(1S) \rightarrow \gamma X$ to have helicity $\pm\lambda$. Because of the normalization condition, the $\theta_h - \theta_\gamma$ probability distribution can be described by two free parameters, traditionally chosen to be the helicity production ratios,

$$x^2 = \frac{|a_1|^2}{|a_0|^2}, \text{ and } y^2 = \frac{|a_2|^2}{|a_0|^2}.$$

To measure x^2 and y^2 , we simultaneously fit the data to the individual θ_h and θ_γ distribu-

⁶ Some authors use a probability distribution that also depends on a third angle, ϕ_h [45]. However, extreme care must be taken when using this angle because it makes the probability distribution sensitive to the relative phases of the helicity amplitudes. Thus, two new free parameters need to be introduced in such a probability distribution, as was noted by [48] and correctly implemented by [44, 45]. Otherwise, the measurement of the helicity amplitudes rests on the assumption that their relative phases are 0 [41, 43, 70, 71].

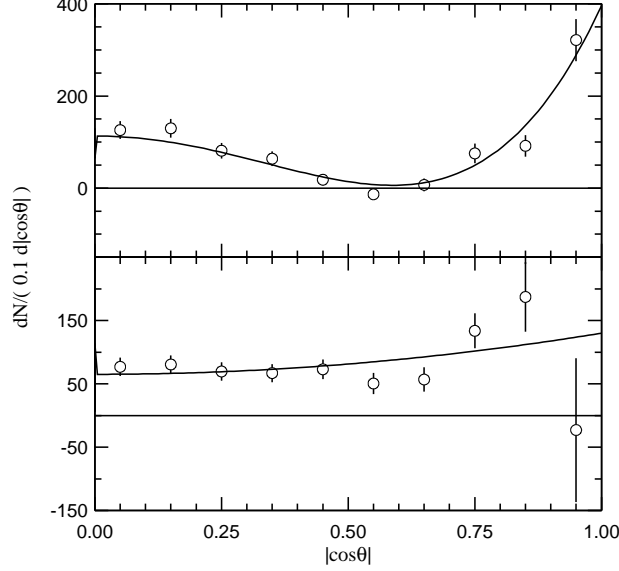


FIG. 8: Distributions of $|\cos \theta_\pi|$ (top) and $|\cos \theta_\gamma|$ (bottom) for the signal events in the $f_2(1270)$ invariant mass region. The solid lines correspond to a simultaneous fit to the $J = 2$ helicity formalism prediction (Equation 3).

tions⁷,

$$\begin{aligned}
 \frac{dN_{\theta_\gamma}}{d \cos \theta_\gamma} &= N \int_{\theta_h} dP_{\theta_h, \theta_\gamma} \\
 &= \frac{N}{1 + x^2 + y^2} \left[x^2 \frac{3}{4} \sin^2 \theta_h + (1 + y^2) \frac{3}{8} (1 + \cos^2 \theta_\gamma) \right] \\
 \frac{dN_{\theta_h}}{d \cos \theta_h} &= N \int_{\theta_\gamma} dP_{\theta_h, \theta_\gamma} \\
 &= \frac{N}{1 + x^2 + y^2} \left[\frac{5}{8} (3 \cos^2 \theta_h - 1)^2 + x^2 \frac{15}{16} \sin^2 2\theta_h + y^2 \frac{15}{16} \sin^4 \theta_h \right],
 \end{aligned} \tag{3}$$

Where N corresponds to the number of events. Using the fits to the data (see Figures 8 and 9) we measure the following helicity production ratios,

$$\begin{aligned}
 x_{f_2(1270)}^2 &= 0.00_{-0.00}^{+0.02}, & y_{f_2(1270)}^2 &= 0.09_{-0.07}^{+0.08}, \\
 x_{f_2'(1525)}^2 &= 0.00_{-0.00}^{+0.10}, & y_{f_2'(1525)}^2 &= 0.30_{-0.17}^{+0.22}.
 \end{aligned}$$

Where only statistical errors are included. These results indicate that both resonances are predominantly produced with helicity 0. They are in agreement with the predictions of [2], and in good agreement with the twist-two order predictions of [3]: no $\lambda = 1$ production, and $\lambda = 2$ production suppressed by a factor of $(m_X/m_b)^2$ with respect to $\lambda = 0$ production, where m_X is the mass of the tensor meson and m_b is the mass of the b quark.

⁷ We choose to use a simultaneous fit to these two distributions instead of a two-dimensional fit using Equation 2 because of our limited statistics.

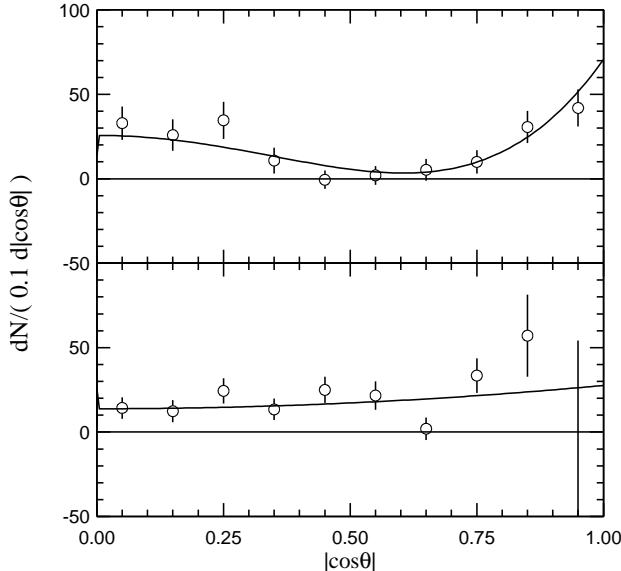


FIG. 9: Distributions of $|\cos \theta_K|$ (top) and $|\cos \theta_\gamma|$ (bottom) for the signal events in the $f_2'(1525)$ invariant mass region. The solid lines correspond to a simultaneous fit to the $J = 2$ helicity formalism prediction (Equation 3).

We use the results from fitting the angular distributions to correct the Monte Carlo simulation efficiencies, which are calculated using flat distributions in the relevant angles, by a factor of 0.78 ± 0.02 for the $f_2(1270)$, 0.90 ± 0.01 for the $f_2'(1525)$, and $0.88_{-0.01}^{+0.03}$ for the significant excess in the $2 - 3 \text{ GeV}/c^2$ region of the di-kaon invariant mass. The large correction in the pion mode is due to the necessarily stronger muon suppression requirement. The measured branching ratios of the significant resonances are,

$$\begin{aligned} \mathcal{B}(\Upsilon(1S) \rightarrow \gamma f_2(1270)) &= (10.2 \pm 0.8 \pm 0.7) \times 10^{-5} \\ \mathcal{B}(\Upsilon(1S) \rightarrow \gamma f_2'(1525)) &= (3.7_{-0.7}^{+0.9} \pm 0.8) \times 10^{-5}, \end{aligned}$$

and the measured branching ratio of the significant excess of events in $\Upsilon(1S) \rightarrow \gamma K^+ K^-$ with a di-kaon invariant mass between $2 - 3 \text{ GeV}/c^2$ is,

$$\mathcal{B}(\Upsilon(1S) \rightarrow \gamma K^+ K^-) = (1.14 \pm 0.08 \pm 0.10) \times 10^{-5},$$

where the first error is statistical and the second includes the systematic uncertainty. The sources of systematic uncertainty are 1% from the number of $\Upsilon(1S)$ decays, 2% from the Monte Carlo simulation of the track reconstruction, 3% (8%) from the Monte Carlo efficiency modeling of the event requirements in the pion (kaon) mode, and 1% to 3% from the uncertainty in the angular distribution measurements. We also assign a 15% systematic uncertainty from possible interference with $\gamma f_2(1270)$ to $\gamma f_2'(1525)$, and less than a 1% systematic uncertainty from high-momentum neutral pions faking photons in the decay $\Upsilon(1S) \rightarrow \rho\pi$ based on the upper limit in [72]. Finally, we include the uncertainties in the $f_2(1270)$ and $f_2'(1525)$ hadronic branching ratios [40] in the systematic uncertainty. For our less significant signal candidates, the branching fraction central value, along with its significance and 90% confidence level upper limit, is shown in Table I.

TABLE I: Branching fraction central value (BF), its statistical significance, and its 90% confidence level upper limit (UL), for each signal candidate with a significance $< 5\sigma$. In the branching fraction central value, the first uncertainty is statistical and the second is systematic. The first three table entries are product branching fractions.

Channel	BF $\times (10^{-5})$	Significance	UL $\times (10^{-5})$
$\gamma f_0(980) \times f_0(980) \rightarrow \pi^+\pi^-$	$1.8_{-0.7}^{+0.8} \pm 0.1$	4.3σ	< 3
$\gamma f_4(2050) \times f_4(2050) \rightarrow \pi^+\pi^-$	$0.37 \pm 0.14 \pm 0.03$	2.6σ	< 0.6
$\gamma f_0(1710) \times f_0(1710) \rightarrow K^+K^-$	$0.38 \pm 0.16 \pm 0.04$	3.2σ	< 0.7
$\gamma p\bar{p}, 2 \text{ GeV}/c^2 < m_{p\bar{p}} < 3 \text{ GeV}/c^2$	$0.41 \pm 0.08 \pm 0.10$	4.8σ	< 0.6

V. DETERMINATION OF UPPER LIMITS FOR $f_J(2220)$ AND $X(1860)$ PRODUCTION AND DECAY

To measure upper limits of the product branching ratio for the decays $\Upsilon(1S) \rightarrow \gamma f_J(2220)$ with $f_J(2220) \rightarrow h^+h^-$, we fit the h^+h^- invariant mass plots, shown in Figure 10, using a Breit-Wigner with a peak mass and width fixed at $2.234 \text{ GeV}/c^2$ and $0.017 \text{ GeV}/c^2$, respectively. These are the values from the possible $f_J(2220)$ signal reported by the BES experiment [49], which is considered a candidate for a glueball. To model the general excess of events between 2.0 and $2.5 \text{ GeV}/c^2$ we also use a flat background function in the fit. Although the highest bin in the $p\bar{p}$ plot is indeed in the region of the $f_J(2220)$, the excess (12 ± 5 events) is not significant, and there are no significant signals anywhere in these three plots. To find upper limits for $f_J(2220) \rightarrow h^+h^-$ decays, we fix the area of the Breit-Wigner to different values, minimize the chi-squared from the fit, and give that area a probability proportional $e^{-\chi^2/2}$. These probability distributions are then used to obtain the following 90% confidence level upper limits on the product branching ratio for $f_J(2220)$ production and decay to each mode:

$$\begin{aligned} \mathcal{B}(\Upsilon(1S) \rightarrow \gamma f_J(2200)) \times \mathcal{B}(f_J(2200) \rightarrow \pi^+\pi^-) &< 8 \times 10^{-7}, \\ \mathcal{B}(\Upsilon(1S) \rightarrow \gamma f_J(2200)) \times \mathcal{B}(f_J(2200) \rightarrow K^+K^-) &< 6 \times 10^{-7}, \\ \mathcal{B}(\Upsilon(1S) \rightarrow \gamma f_J(2200)) \times \mathcal{B}(f_J(2200) \rightarrow p\bar{p}) &< 11 \times 10^{-7}. \end{aligned}$$

The systematic uncertainties on the branching ratios were added in quadrature with the statistical errors in forming the above limits. Using the $X(1860)$ parameters measured in [52], and proceeding in a similar manner as described above, we obtain,

$$\mathcal{B}(\Upsilon(1S) \rightarrow \gamma X(1860)) \times \mathcal{B}(X(1860) \rightarrow p\bar{p}) < 5 \times 10^{-7},$$

with a 90% confidence level.

VI. SUMMARY AND CONCLUSION

We have confirmed CLEO's previous observation of the $f_2(1270)$ in radiative $\Upsilon(1S)$ decays and made a new observation of the $f_2'(1525)$, obtaining factors of 0.07 ± 0.01 and $0.08_{-0.03}^{+0.04}$ for the ratio of the $\Upsilon(1S)$ branching fraction with respect to the one measured in J/ψ radiative

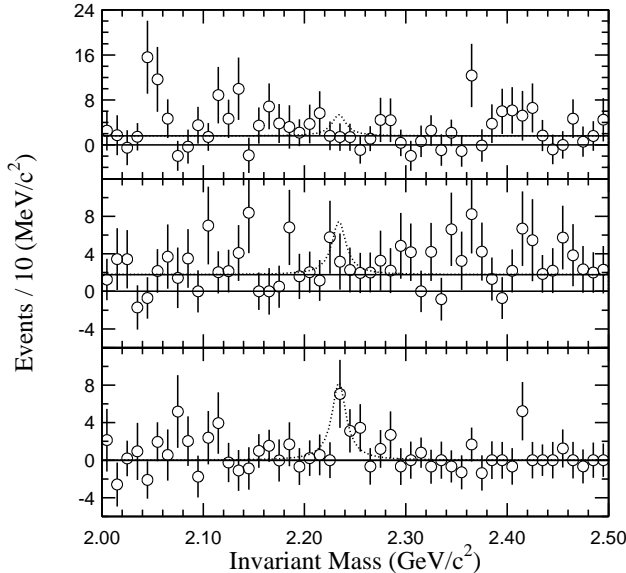


FIG. 10: Invariant mass of $\pi^+\pi^-$ (top) K^+K^- (middle) and $p\bar{p}$ (bottom) from $\Upsilon(1S) \rightarrow \gamma h^+ h^-$ with the fit that determines the 90% C.L. upper limit overlaid. The upper limit is obtained from fits to a $f_J(2220)$ signal Breit-Wigner function (dashed) and flat background function (solid). The flat background function is used to model the excess of events from $\Upsilon(1S) \rightarrow \gamma h^+ h^-$ in this invariant mass region.

decays, respectively. These values are larger than, but the same order of magnitude as, the ratio of 0.04 expected from naive scaling arguments. The observed $f_2(1270)$ production is in agreement with the prediction in [3] and somewhat lower than the prediction in [2]. In both of the measured modes we can confirm by fits to the angular distributions of the photon and charged particles that the two daughter hadrons are indeed produced by a spin-2 parent. We find that this parent is produced mostly with helicity 0, in good agreement with the predictions in [2, 3]. No structure is seen in the $p\bar{p}$ invariant-mass distribution. In particular, we do not observe a near-threshold enhancement as in [52]. Finally, stringent limits have been put on the production of the glueball candidate $f_J(2220)$ in radiative $\Upsilon(1S)$ decays. Glueball production is expected to be enhanced in $\Upsilon(1S)$ radiative decays [22, 73, 74], but we find that, within our experimental sensitivity, tensor meson states, believed to be composed only of quarks, dominate the di-gluon spectrum.

We gratefully acknowledge the effort of the CESR staff in providing us with excellent luminosity and running conditions. This work was supported by the National Science Foundation and the U.S. Department of Energy.

-
- [1] G.T. Bodwin, E. Braaten and G.P. Lepage, Phys. Rev. D **51**, 1125 (1995).
 - [2] S. Fleming, C. Lee and A.K. Leibovich, Phys. Rev. D **71**, 074002 (2005).
 - [3] J.P. Ma, Nucl. Phys. B **605**, 625 (2001).
 - [4] V.N. Baier and A.G. Grozin, Sov. J. Nucl. Phys. **35**, 596 (1982).
 - [5] V.N. Baier and A.G. Grozin, Z. Phys. C **29**, 161 (1985).
 - [6] T. Barnes, Z. Phys. C **10**, 275 (1981).

- [7] J.M. Cornwall and A. Soni, Phys. Lett. B **120**, 431 (1983).
- [8] W.S. Hou and G.G. Wong, Phys. Rev. D **67**, 034003 (2003).
- [9] C.J. Morningstar and M.J. Peardon, Phys. Rev. D **60**, 034509 (1999).
- [10] A. Vacarino and D. Weingarten, Phys. Rev. D **60**, 114501 (1999).
- [11] C. Liu, Chin. Phys. Lett. **18**, 187 (2001).
- [12] D.Q. Liu, J.M. Wu and Y. Chen, High Energy Phys. Nucl. Phys. **26**, 222 (2002).
- [13] P.G.O. Freund and Y. Nambu, Phys. Rev. Lett. **34**, 1645 (1975).
- [14] R.L. Jaffe and K. Johnson, Phys. Lett. B **60**, 201 (1976).
- [15] T. Barnes, F.E. Close and S. Monaghan, Nucl. Phys. B **198**, 380 (1982).
- [16] C.E. Carlson, T.H. Hanson, and C. Peterson, Phys. Rev. D **27**, 1556 (1983).
- [17] N. Isgur and J. Paton, Phys. Rev. D **31**, 2910 (1985).
- [18] S. Narison, Z. Phys. C **26**, 209 (1984).; Nucl. Phys. B **509**, 312 (1998); Nucl. Phys. Proc. Suppl. **96**, 244 (2001).
- [19] M.H. Thomas, M.Lust and H.J. Mang, J. Phys. G **18**, 1125 (1992).
- [20] J.Y. Cui, J.M. Wu and H.Y. Jin, Phys. Lett. B **424**, 381 (1998).
- [21] S.J. Brodsky, A.S. Goldhaber and J. Lee, Phys. Rev. Lett. **91**, 112001 (2003).
- [22] X.G. He, H.Y. Jin and J.P. Ma, Phys. Rev. D **66**, 074015 (2002).
- [23] M. Melis, F. Murgia and J. Parisi, Phys. Rev. D **70**, 034021, (2004).
- [24] J.C. Su and J.X. Chen, Phys. Rev. D **69**, 076002 (2004).
- [25] V.V. Anisovich *et al.* (Crystal Ball Collaboration), Phys. Lett. B **323**, 233 (1994).
- [26] V.V. Anisovich, D.V. Bugg, A.V. Sarantsev and B.S. Zou, Phys. Rev. D **50**, 1972 (1994).
- [27] C. Amsler *et al.* (Crystal Barrel Collaboration), Phys. Lett. B **355**, 425 (1995).
- [28] C.A. Meyer, "Proceedings of the Workshop on Gluonic Excitations," Newport News, Virginia 2003, AIP Conf. Proc. **698**, 554 (2004).
- [29] K.K. Seth, Nucl. Phys. B (Proc. Suppl.) **96**, 205 (2001).
- [30] Bing-Song Zou, Nucl. Phys. **A644**, 41c (1999).
- [31] C. Amsler and F.E. Close, Phys. Lett. B **353**, 385 (1995).
- [32] D. Weingarten, Nucl. Phys. Proc. Suppl. **53**, 232 (1997).
- [33] D.V. Bugg, M.J. Peardon and B.S. Zou, Phys. Lett. B **486**, 49 (2000).
- [34] J. Sexton, A. Vacarino and D. Weingarten, Phys. Rev. Lett. **75**, 4563 (1995).
- [35] V.V. Anisovich, Phys. Lett. B **364**, 195 (1995).
- [36] F. Giacosa, T. Gutsche and A. Faessler, Phys. Rev. C **71**, 025202 (2005).
- [37] M. Chanowitz, hep-ph/0506125.
- [38] A.H. Fariborz, Int. J. Mod. Phys. A **19**, 5417 (2004).
- [39] N. Brambilla *et al.*, hep-ph/0412158.
- [40] S. Eidelman *et al.*, (Particle Data Group Collaboration), Phys. Lett. B **592**, 1 (2004).
- [41] G. Alexander *et al.* (Pluto Collaboration), Phys. Lett. B **76**, 652 (1978).
- [42] D.L. Scharre, "10th International Symposium on Lepton and Photon Interactions at High Energy", Bonn (1981).
- [43] C. Edwards *et al.* (Crystal Ball Collaboration), Phys. Rev. D **25**, 3065 (1982).
- [44] J.E. Augustin *et al.* (DM2 Collaboration), Z. Phys. C **36**, 369 (1987).
- [45] R.M. Baltrusaitis *et al.* (Mark III Collaboration), Phys. Rev. D **35**, 2077 (1987).
- [46] J.Z. Bai *et al.* (BES Collaboration), Phys. Rev. D **68**, 052003 (2003).
- [47] M. Krammer, Phys. Lett. B **74**, 361 (1978).
- [48] J.G. Korner, J.H. Kuhn, M. Krammer and H. Schneider, Nucl. Phys. B **229**, 115 (1983).
- [49] J.Z. Bai *et al.*, (BES Collaboration), Phys. Rev. Lett. **76**, 3502 (1996).

- [50] R.M. Baltrusaitis *et al.* (MARK-III Collaboration), Phys. Rev. Lett. **56**, 107 (1986).
- [51] J.E. Augustin *et al.* (DM2 Collaboration), Phys. Rev. Lett. **60**, 2238 (1988).
- [52] J.Z. Bai *et al.* (BES Collaboration), Phys. Rev. Lett. **91**, 022001 (2003).
- [53] A. Sibirtsev, J. Haidenbauer, S. Krewald, U.G. Meissner and A.W. Thomas, Phys. Rev. D **71**, 054010 (2005).
- [54] B. Kerbikov, A. Stavinsky and V. Fedotov, Phys. Rev. C **69**, 055205 (2004).
- [55] D.V. Bugg, Phys. Lett. B **598**, 8 (2004).
- [56] C.S. Gao and S.L. Zhu, Commun. Theor. Phys. **42**, 844 (2004).
- [57] B.S. Zou and H.C. Chiang, Phys. Rev. D **69**, 034004 (2004).
- [58] B. Loiseau and S. Wycech, hep-ph/0501112.
- [59] G.J. Ding and M.L. Yan, hep-ph/0502127.
- [60] A. Anastassov *et al.*, (CLEO Collaboration), Phys. Rev. Lett. **82**, 286 (1999).
- [61] G. Masek *et al.*, (CLEO Collaboration), Phys. Rev. D **65**, 072002 (2002).
- [62] L. Breva-Newell, Ph.D. Thesis, University of Florida, hep-ex/0412075.
- [63] G. Viehhauser, Nucl. Inst. Meth. A **462**, 146 (2001); D. Peterson *et al.*, Nucl. Inst. Meth. A **478**, 142 (2002); A. Warburton *et al.*, Nucl. Inst. and Meth. A **488**, 451 (2002); M. Artuso *et al.*, physics/0506132.
- [64] R.A. Briere *et al.*, (CLEO Collaboration), Phys. Rev. D **70**, 072001 (2004).
- [65] *QQ - The CLEO Event Generator*, <http://www.lns.cornell.edu/public/CLEO/soft/qq> (unpublished).
- [66] R. Brun *et al.*, GEANT 3.15, CERN Report No. DD/EE/84-1 (1987).
- [67] T. Sjöstrand, Comput. Phys. Commun. **82**, 74 (1994); T. Sjöstrand and M. Bengtsson *ibid* **43**, 367 (1987); T. Sjöstrand, *ibid* **39**, 347 (1986).
- [68] M.A. Selen, R.M. Hans and M.J. Haney, IEEE Trans. Nucl. Sci. **48**, 562 (2001).
- [69] J.D. Richman CALT-68-1148 (1995) (unpublished).
- [70] P.K. Kabir and A.J.G. Hey, Phys. Rev. D **13**, 3161 (1976).
- [71] M. Ablikim *et al.* (BES Collaboration), Phys. Rev. D **70**, 092004 (2004)
- [72] S.A. Dytman (CLEO Collaboration), hep-ex/0307035.
- [73] S. Godfrey and J. Napolitano, Rev. Mod. Phys. **71**, 1411 (1999).
- [74] F.E. Close, G.R. Farrar and Z.p. Li, Phys. Rev. D **55**, 5749 (1997).